

**UCLA**

**UCLA Electronic Theses and Dissertations**

**Title**

Solvation Effects on Acid-Catalyzed Reaction Paths of Propionaldehyde in the Liquid Phase

**Permalink**

<https://escholarship.org/uc/item/43c7x32k>

**Author**

LI, QI

**Publication Date**

2017

Peer reviewed|Thesis/dissertation

UNIVERSITY OF CALIFORNIA

Los Angeles

Solvation Effects on Acid-Catalyzed Reaction Paths  
of Propionaldehyde in the Liquid Phase

A thesis submitted in partial satisfaction  
of the requirements for the degree Master of Science  
in Chemical Engineering

by

Qi Li

2017

© Copyright by

Qi Li

2017

## ABSTRACT OF THE THESIS

### Solvation Effects on Acid-Catalyzed Reaction Paths of Propionaldehyde in the Liquid Phase

by

Qi Li

Master of Science in Chemical Engineering

University of California, Los Angeles, 2017

Professor Dante A. Simonetti, Chair

Aldol condensations are one of the most important methods to form carbon-carbon bonds in organic chemistry and biochemistry. The kinetics of formation of the 2-methyl-2-pentenal in acid-catalyzed aldol condensation reaction of propionaldehyde were studied at ambient temperature and 175°C in pure water and a mixture consisting of 80 vol%  $\gamma$ -valerolactone (GVL) and 20 vol% water using aqueous HCl and on various solid acid zeolites. The reaction was determined to be second order in propionaldehyde. The rate constants for the reaction at ambient temperature with 0.2M HCl solution as catalyst using pure water and 80/20 GVL/H<sub>2</sub>O were 0.0131 and 0.0183  $M^{-1}s^{-1}$  respectively, showing that GVL as a co-solvent enhances the reaction rate via solvation of the aldol-condensation reaction transition state.

Propionaldehyde conversions and selectivities to 2-methyl-2-pentenal varied on the different zeolites tested (BEA, Y, MOR, MFI, FER) at 175°C using both water and 80/20 GVL/H<sub>2</sub>O as solvents. The conversions of propionaldehyde range from 13.9% (MOR using GVL/H<sub>2</sub>O as solvent) to 85.7% (MFI using water as solvent). Among the six products formed during propionaldehyde conversion (acetaldehyde, ethanol, C<sub>4</sub> ketones, C<sub>6</sub> acids, C<sub>6</sub> aldehydes, and C<sub>9+</sub> molecules), C<sub>6</sub> aldehydes are the predominant product (39% for Y-SiO<sub>2</sub>/Al<sub>2</sub>O<sub>3</sub> ratio=15 in GVL/H<sub>2</sub>O, 40% for Y-SiO<sub>2</sub>/Al<sub>2</sub>O<sub>3</sub> ratio=2.6 in water, 57% and 56% for MFI in GVL/H<sub>2</sub>O and in water respectively, 25% and 49% for FER in GVL/H<sub>2</sub>O and in water respectively, 21% and 44% for MOR in GVL/H<sub>2</sub>O and in water respectively, 50% and 84% for BEA in GVL/H<sub>2</sub>O and in water respectively) except Y-SiO<sub>2</sub>/Al<sub>2</sub>O<sub>3</sub> ratio=15 in water (8%) and Y-SiO<sub>2</sub>/Al<sub>2</sub>O<sub>3</sub> ratio=2.6 in GVL/H<sub>2</sub>O (14%). All of the zeolites tested facilitated cracking reactions of C<sub>6</sub> aldehydes to produce acetaldehyde and ethanol (25% and 93% for Y-SiO<sub>2</sub>/Al<sub>2</sub>O<sub>3</sub> ratio=15 in GVL/H<sub>2</sub>O and water respectively, 25% and 60% for Y-SiO<sub>2</sub>/Al<sub>2</sub>O<sub>3</sub> ratio=2.6 in GVL/H<sub>2</sub>O and water respectively, 36% and 24% for MFI in GVL/H<sub>2</sub>O and water respectively, 48% and 51% for FER in GVL/H<sub>2</sub>O and water respectively, 78% and 56% for MOR in GVL/H<sub>2</sub>O and water respectively, 50% and 12% for BEA in GVL/H<sub>2</sub>O and water respectively). C<sub>4</sub> ketones only appear when Y and MFI are used as catalyst (12% for Y-SiO<sub>2</sub>/Al<sub>2</sub>O<sub>3</sub> ratio=2.6 in GVL/H<sub>2</sub>O, 7% and 9% for MFI in GVL/H<sub>2</sub>O and water respectively). Further, Y and FER zeolites appear to facilitate oxidation reaction as evidenced by the formation of C<sub>6</sub> acids (35% for Y-SiO<sub>2</sub>/Al<sub>2</sub>O<sub>3</sub> ratio=15 in GVL/H<sub>2</sub>O, 48% for Y-SiO<sub>2</sub>/Al<sub>2</sub>O<sub>3</sub> ratio: 2.6 in GVL/H<sub>2</sub>O, 27% for FER in water).

Conversions using water as solvent were 1.5-4.3 times larger than using GVL/H<sub>2</sub>O as solvent for all catalysts tested except Y-SiO<sub>2</sub>/Al<sub>2</sub>O<sub>3</sub> ratio=15, which had similar conversions for both solvents. Selectivities to the aldol condensation product using water as solvent were 1.7-2.7 times larger than using GVL/H<sub>2</sub>O as solvent for all catalysts tested except Y-SiO<sub>2</sub>/Al<sub>2</sub>O<sub>3</sub> ratio=15. In addition, water facilitated aromatization reactions for C<sub>9+</sub> molecules on MFI (4%) and BEA (4%).

The thesis of Qi Li is approved.

Panagiotis D. Christofides

Philippe Sautet

Dante A. Simonetti, Committee Chair

University of California, Los Angeles

2017

## Table of Contents

Chapter 1. Introduction	1-3
Chapter 2. Background	4-5
Chapter 3. Experimental	6-7
Chapter 4. Results and Discussion	
4.1 Initial rates and rate order determinations at ambient temperature	8-11
4.2 Conversion and selectivity on solid catalysts at high temperature	11-15
Chapter 5. Conclusion	16
Reference	17-18



## List of Figures, Tables, and Schemes

Scheme 1-1	3
Reaction network for the acid-catalyzed condensation of propionaldehyde	
Figure 4.1-1	9
Propionaldehyde concentration versus reaction time plot using 0.2M HCl as catalyst and water as solvent at 25°C	
Figure 4.1-2	9
Propionaldehyde concentration versus reaction time plot using 0.2M HCl as catalyst and GVL/H <sub>2</sub> O as solvent at 25°C	
Figure 4.1-3	10
Initial rates for the aldol condensation reaction of propionaldehyde versus initial propionaldehyde concentration using 0.2M HCl as catalyst and using water and 80/20 GVL/H <sub>2</sub> O as solvent at 25°C	
Figure 4.2-1	12
Conversions of propionaldehyde in the reaction of propionaldehyde with an initial concentration of 0.2 M, using BEA, Y-SiO <sub>2</sub> /Al <sub>2</sub> O <sub>3</sub> ratio:15, Y-SiO <sub>2</sub> /Al <sub>2</sub> O <sub>3</sub> ratio:2.6, MFI, MOR, and FER as catalyst in both solvents: GVL/H <sub>2</sub> O and pure water at 175°C for 2 hours	
Figure 4.2-2	12
Molecular structure of $\gamma$ -valerolactone (GVL)	
Figure 4.2-3	13
Selectivities to ethanol, acetaldehyde, C <sub>4</sub> ketones, C <sub>6</sub> acids, C <sub>6</sub> aldehydes, and C <sub>9</sub> + in the reaction of propionaldehyde with an initial concentration of 0.2 M, using BEA, Y-SiO <sub>2</sub> /Al <sub>2</sub> O <sub>3</sub> ratio:15, Y-SiO <sub>2</sub> /Al <sub>2</sub> O <sub>3</sub> ratio:2.6, MFI, MOR, and FER as catalyst in both solvents: GVL/H <sub>2</sub> O and pure water at 175°C for 2 hours	

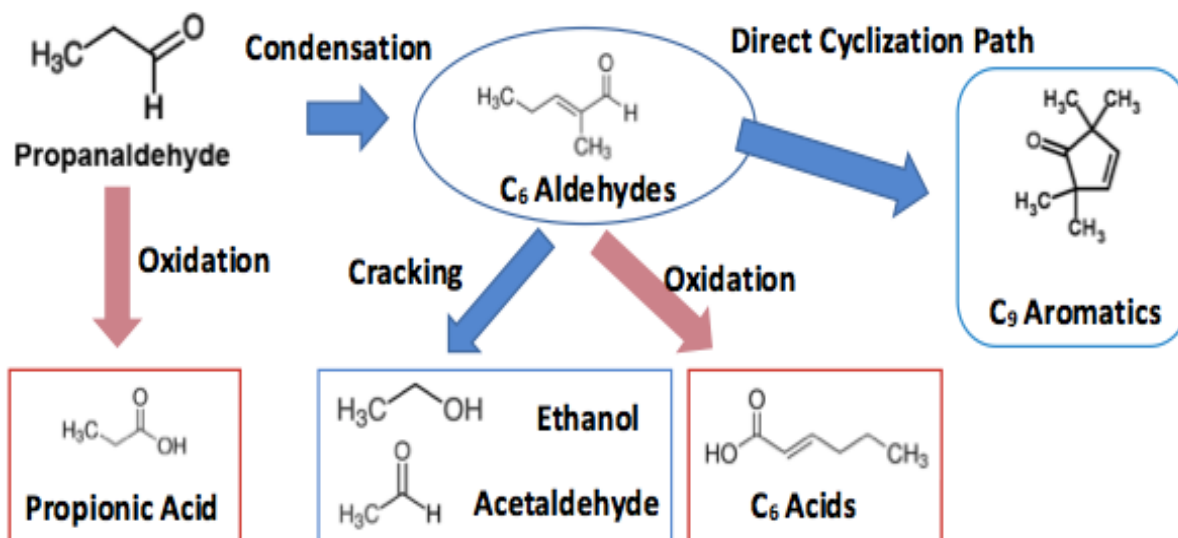
## Chapter 1. Introduction

Every living matter on earth is a source of biomass, including plant materials such as algae, grass and crops or animal product such as manure <sup>[1]</sup>. As one of the most important energy source, biomass provides 10-14% of the world total energy <sup>[2]</sup>. After undergoing various processes, biomass can be converted into several useful forms of energy. The most important product of biomass conversion is hydrogen. There are three common routes of hydrogen production from biomass: fermentative production, photosynthesis, and biological water gas shift reaction <sup>[3]</sup>. Another important product is the hydrocarbon fuel. The general strategy of hydrocarbon fuel production is to decrease the feedstock oxygen content to improve energy density and to form C–C bonds between biomass-derived intermediates which lead to a lighter hydrocarbon product <sup>[4]</sup>. One specific example is the conversion of lignocellulosic biomass. Upon the removal of oxygen content and formation of C–C bonds, only the least amount of hydrogen from external source is required, such as the product from steam methane reforming. The conversion consists of two steps: (1) conversion of the solid lignocellulosic biomass feedstock to a gas-phase or liquid-phase chemical platform, partially removing oxygen <sup>[4]</sup>; and (2) catalytic upgrading of this chemical platform to the final hydrocarbon fuel by controlled carbon-carbon coupling reactions and removal of the remaining oxygen functionality <sup>[4]</sup>.

One useful application of the conversion of biomass is the production of organic solvent. In the industry, a wide range of organic solvents are used including cleaning solutions, adhesives, etc. It has been recently shown that the adoption of organic solvent can greatly improve the performance of propionaldehyde coupling process. Since propionaldehyde

plays a critical role as the intermediate and processing aid for the manufacturing industry, it is ideal to find the most suitable solvent to enhance the production. One of the biomass conversion products is  $\gamma$ -valerolactone (GVL), which has been proved to improve the reaction performance such as increased catalytic activity and higher selectivity to desired reaction products<sup>[5]</sup>. Also, the accelerated rates of propionaldehyde conversion in GVL/H<sub>2</sub>O mixture are used to produce C<sub>6</sub> molecules in some developed process strategies.

In the work presented herein, propionaldehyde condensation was studied in the liquid phase at 175°C on BEA, MFI (ZSM-5), MOR, FER, and two Y zeolites with different Si/Al ratios using water and a mixture of GVL/H<sub>2</sub>O as solvents. The results from these solid acid catalysts were compared to propionaldehyde condensation reactions in aqueous HCl under ambient conditions (25°C and 1atm). Scheme 1 shows a simplified reaction network for the conversion of propionaldehyde on acid catalysts. The catalytic conversion of propionaldehyde into 2-methyl-2-pentenal through condensation is accompanied by various reactions, producing undesired side products through four main path ways: ring formation to C<sub>9</sub> molecules after 2-methyl-2-pentenal reacts with propionaldehyde to form 2,4-dimethyl-2,4-heptadienal, oxidation to form propionic acid, cracking of C<sub>6</sub> molecules to form acetaldehyde, ethanol, and C<sub>6</sub> acids. The results presented in this study indicate that different solvent environments increase the rate of formation of condensation product in homogeneous catalysis systems. However, these effects of solvation may be mitigated by diffusional restrictions within solid zeolites, where spatial constraints dictate reaction paths and product selectivities.



**Scheme 1-1:** Reaction network for the acid-catalyzed condensation of propionaldehyde.

## Chapter 2. Background

Biomass is a major source of sustainable energy for our society. In the past few decades, scholarly efforts have been emphasized on the liquid phase biomass conversion through fundamental reactions including oxidation, reforming, isomerization, hydrolysis, aldol condensation, dehydration, and hydrogenation. In the past study by Luterbacher, et al., which focuses on breaking down cellulose and hemicellulose, a yield of 70% - 90% is reported for the production of soluble carbohydrates from materials such as corn stover, hardwood, and softwood using a mixture of GVL, H<sub>2</sub>O, and dilute H<sub>2</sub>SO<sub>4</sub> [5].

An important reaction to be discussed is the Aldol condensation, where C-C bond is formed to construct large molecules at relatively mild temperatures using various acid catalysts. Because aldol condensation reaction is a well-known acid-catalyzed reaction, a number of studies have compared between the performance of aldehydes incorporation into acidic solutions and that into non-acidic solutions. Similar studies have been performed for ketones, acrolein, apinene, and isoprene [6]. The heterogeneous interactions of aldehydes with sulfuric acid surfaces have also been studied in the past. However, in some of these studies, the authors found it difficult to identify the specific molecular products. Therefore, in these studies, analytical methods were used to target the specific product. For example, Mia et al. [6] used UV-Vis to show that aliphatic aldehydes undergo aldol condensation reactions on sulfuric acid aerosols under laboratory conditions, despite the fact that they used relatively high concentrations of sulfuric acid (60wt% - 85wt%).

The effects of GVL as a facilitative solvent in acid-catalyzed reactions have also been

widely discussed. For example, the high yield of the conversion from cellulose to levulinic acid is observed. When using GVL as the solvent together with Amberlyst 70 as the catalyst, the yield is improved from 20%, when using water as the solvent, to 70% under the same condition. In two other studies by Zhang, et al.<sup>[8]</sup> and Li, et al.<sup>[9]</sup>, when GVL is used as a solvent, an increased selectivity is observed for the conversion of C<sub>5</sub> and C<sub>6</sub> sugars to their corresponding furanic components: furfural and 5-hydroxymethylfurfural (HMF) <sup>[10]</sup>. Moreover, Mellmer, et al. studied the solvent effect of GVL in the dehydration of 1,2-propanediol at 448 K using sulfuric acid as catalyst. It is shown in their study that, when compared to using water as solvent, the reactivity of 1,2-propanediol conversion is increased by 18 times and the selectivity to propionaldehyde is increased by 25% <sup>[11]</sup>. They also showed that, in a separate set of experiments, using GVL as solvent increased reaction rates of acid-catalyzed biomass hydrolysis, while in the meantime lowered the apparent activation energy for biomass hydrolysis by about 40% <sup>[10]</sup>. Therefore, the conversion of monosaccharide is increased, which leads to a higher thermodynamic feasibility for monosaccharide production from biomass <sup>[10]</sup>.

### Chapter 3. Experimental

Propionaldehyde (purchased from Acros Organics with a purity of 99+%), hydrochloric acid (purchased from VWR Analytical with a purity of 35 wt%-37.5 wt%), and  $\gamma$ -valerolactone (purchased from Alfa Aesar with a purity of 98+%) were used without further purification. Hydrochloric acid was diluted into 0.5M and 1 M solutions. Zeolites BEA ( $\text{SiO}_2/\text{Al}_2\text{O}_3$  ratio:12.5), Y ( $\text{SiO}_2/\text{Al}_2\text{O}_3$  ratio:15), Y ( $\text{SiO}_2/\text{Al}_2\text{O}_3$  ratio:2.6), MOR ( $\text{SiO}_2/\text{Al}_2\text{O}_3$  ratio:10), and FER ( $\text{SiO}_2/\text{Al}_2\text{O}_3$  ratio:10), and MFI (ZSM-5,  $\text{SiO}_2/\text{Al}_2\text{O}_3$  ratio:11.5) were purchased from Zeolyst International in the ammonium form and converted to the proton form by treatment in air for 10 hours at 600°C with a ramp rate of 1°C/min.

Reactions were carried out at ambient temperature and pressure inside of 10 mL glass scintillation vials. Aqueous solutions of propionaldehyde were prepared by adding pure propionaldehyde to deionized water or 80/20 (volume) GVL/ $\text{H}_2\text{O}$  mixture. The hydrochloric acid solutions were prepared by dilution of concentrated (35 wt%-37.5 wt%) HCl with deionized water. Then, the solutions of propionaldehyde were added to the HCl solution and mixing for several minutes to ensure solution homogeneity<sup>[6]</sup>. A small portion of the reaction mixture was then added to the 10mL vial and then was injected into GC-MS to identify products after specific time intervals. GC-MS analyses were performed on an Agilent Technologies 7890B GC system and an Agilent Technologies 5977A MSD.

Reactions at 175 °C were performed in 25mL thick-walled glass reactor under autogeneous pressure. 4mL of solution with ~72 $\mu\text{L}$  propionaldehyde, appropriate amount of solvent, and 50mg catalyst were added into the reactor. The reactors were placed in an oil

bath at the desired reaction temperature and stirred at 200 rpm. Reactors were removed from the oil bath at specific reaction times and cooled by flowing compressed air. After reaction, the content of the reactor was filtered using a 0.2 $\mu$ m membrane (purchased from VWR International). Small portions (0.4  $\mu$ L) of the solutions after reaction were injected into GC-MS to identify products and quantify for concentration.

The initial rate method was used to determine the rate order and rate constant for the aldol condensation reaction of propionaldehyde using HCl. A power law rate expression was used in the batch reactor mass balance for propionaldehyde according to Equation 3-1:

$$\frac{d[\text{propional}]}{dt} = -2k[\text{propional}]^n = -2k[\text{propional}]_0^n \quad (3-1)$$

Equation 3-1 can be linearized to determine the rate order  $n$ , and the rate constant  $k$ , as shown in 3-2:

$$\log\left(\frac{d[\text{propional}]}{dt}\right) = -n\log[\text{propional}] + \log(2k) \quad (3-2)$$

The reaction order  $n$  and reaction rate  $k$  can be determined from the log-log plot of initial rate of propionaldehyde conversion versus initial concentration of propionaldehyde.



## Chapter 4. Results and Discussion

### 4.1 Initial rates and rate order determinations at ambient temperature

The initial rate method was used to determine the rate order and rate constant for the aldol condensation reaction of propionaldehyde at ambient temperature. Figure 4.1-1 shows the decrease in the aldol concentrations in the reactor with reaction time for different initial concentrations of aldehyde (0.1 M, 0.15 M, 0.2 M, and 0.25 M) at ambient temperature (~25°C) using water as solvent and 0.2 M HCl as catalyst. Figure 4.1-2 shows the decrease in the aldol concentrations in the reactor with reaction time for different initial concentrations of aldehyde (0.1 M, 0.2 M, 0.3 M, and 0.4 M) at ambient temperature (~25°C) using 80/20 GVL/H<sub>2</sub>O mixture as solvent and 0.2 M HCl as catalyst. The initial rates determined from the data in Figure 4.1-1 and Figure 4.1-2 are shown in Figure 4.1-3 for the various initial propionaldehyde concentrations. From Figure 4.1-3, a rate order of 1.96 and a rate constant of  $0.0131 (s \cdot M)^{-1}$  were determined when water is the solvent while a rate order of 1.97 and a rate constant of  $0.0183 (s \cdot M)^{-1}$  were determined using 80/20 GVL/H<sub>2</sub>O mixture as solvent.

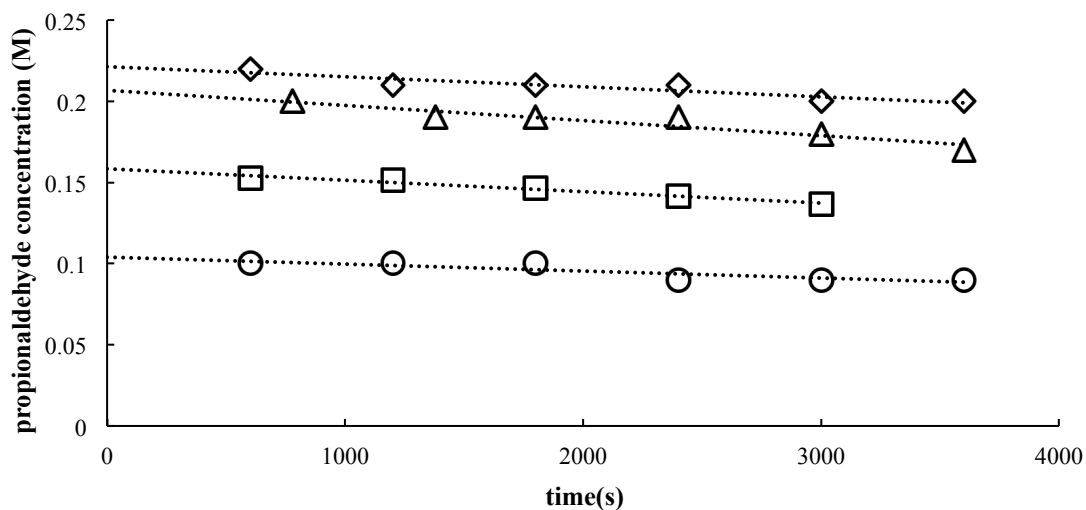


**Figure 4.1-1:** Propionaldehyde concentration versus reaction time plot. The slope of each line is the initial rate for the aldol condensation reaction of propionaldehyde at following initial concentrations using 0.2M HCl as catalyst and water as solvent at 295 K: circles:  $[\text{propionaldehyde}]_0=0.1\text{M}$ , squares:  $[\text{propionaldehyde}]_0=0.15\text{M}$ , triangles:  $[\text{propionaldehyde}]_0=0.2\text{M}$ , and diamonds:  $[\text{propionaldehyde}]_0=0.25\text{M}$ .

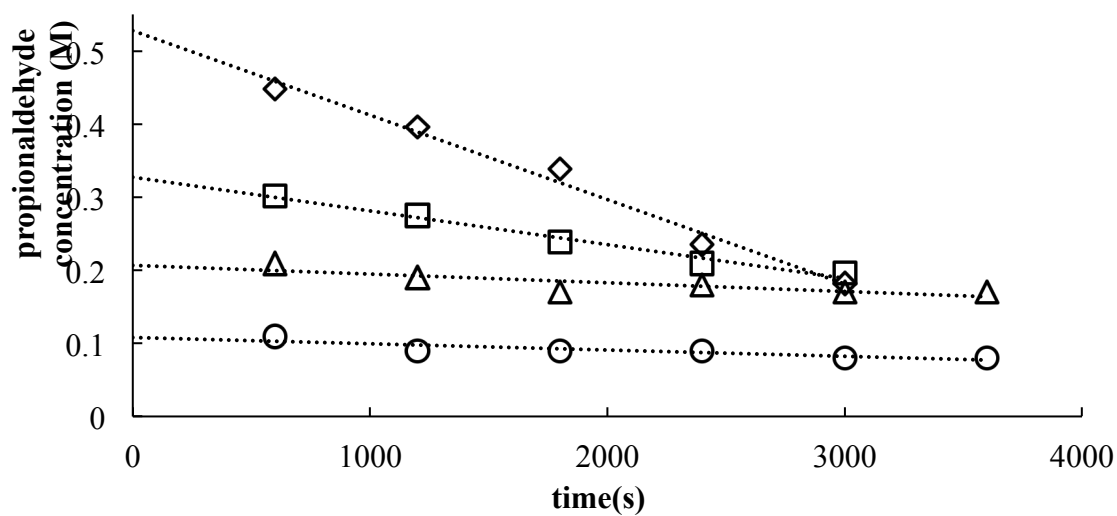


**Figure 4.1-2:** Propionaldehyde concentration versus reaction time plot. The slope of each line is the initial rate for the aldol condensation reaction of propionaldehyde at following initial concentrations using 0.2M HCl as catalyst and 80/20 GVL/H<sub>2</sub>O as solvent at 295K: circles:  $[\text{propionaldehyde}]_0=0.1\text{M}$ , triangles:  $[\text{propionaldehyde}]_0=0.2\text{M}$ , squares:  $[\text{propionaldehyde}]_0=0.3\text{M}$ , and diamonds:  $[\text{propionaldehyde}]_0=0.4\text{M}$ .

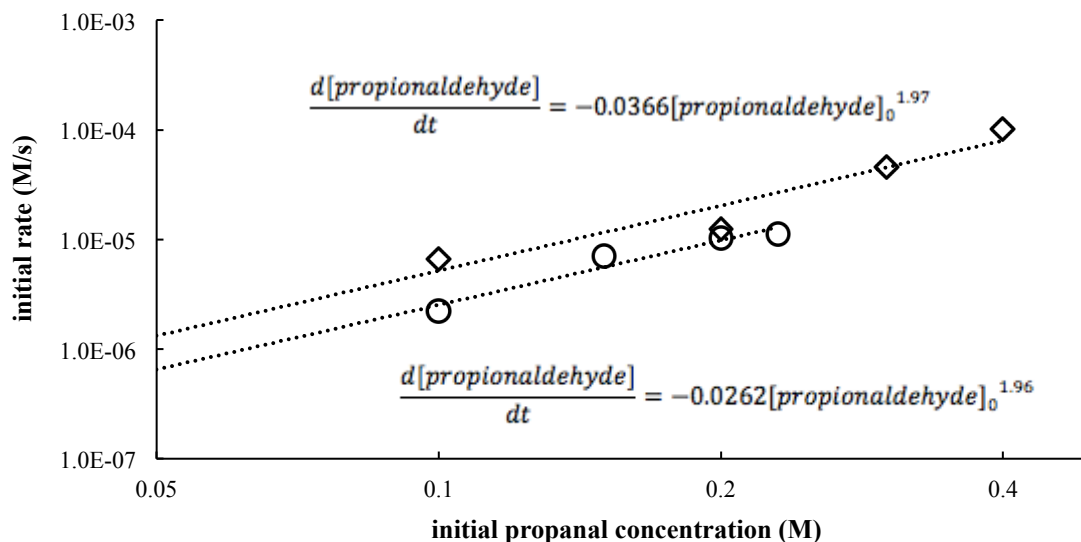


**Figure 4.1-3:** Initial rates for the aldol condensation reaction of propionaldehyde versus initial propionaldehyde concentration using 0.2M HCl as catalyst and using water and 80/20 GVL/H<sub>2</sub>O as solvent. Circles: using water as solvent; Diamonds: using 80/20 GVL/H<sub>2</sub>O as solvent.

The aldol condensation reaction was second order in propionaldehyde in both water (1.96) and GVL/H<sub>2</sub>O mixture (1.97) in agreement with previous studies <sup>[6]</sup>. The measured rate constant  $k$  represents the intrinsic rate constant times the hydrochloric acid concentration. Therefore the intrinsic rate constants can be determined from the measured rate constant and the concentration of acid. These values were  $0.0655 \text{ s}^{-1}\text{M}^{-1}$  and  $0.0915 \text{ s}^{-1}\text{M}^{-1}$  using water and 80/20 GVL/H<sub>2</sub>O as solvent, respectively. The reaction rate constant using 80/20 GVL/H<sub>2</sub>O as the solvent is 1.4 times higher than the rate constant using pure water as the solvent, indicating a moderate solvation effect. However, Mellmer et al. showed a much larger solvation effect (~18 times <sup>[11]</sup>) for the 1,2-propanediol dehydration reaction using sulfuric acid as catalyst at 403 K. There are two possible reasons for the modest solvation effect shown in Figure 4.1-3. First, the transition state that is formed during aldol condensation reaction could be less sensitive to solvation than the dehydration reaction

transition state. However, the transition states of both reactions are likely to be cationic species with positive charge on a secondary carbon atom, thus, the solvent will likely stabilize these transition states to similar extents.<sup>[12]</sup> An alternative explanation is that the Gibbs free energy of solvation is smaller at ambient temperature than that at higher temperatures. McGrath, et al. calculated the Gibbs free energies of solvation and dissociation of HCl in water at 4 temperatures between 300 K and 450 K<sup>[13]</sup>. They showed a temperature dependence of the Gibbs free energy of solvation of about  $30 \text{ cal mol}^{-1}\text{K}^{-1}$ , meaning that an increase of 1 K in temperature raises the Gibbs free energy by  $30 \text{ cal mol}^{-1}$ <sup>[13]</sup>. Therefore, at lower temperatures, the Gibbs free energy of solvation is lower and has less of an impact of the energy barrier for the overall reaction.

#### **4.2 Conversion and selectivity on solid catalysts at high temperature**

To probe propionaldehyde reaction on solid acid catalysts (and the effects of bulk phase solvent on heterogeneously catalyzed reactions), reaction kinetics data were collected for propionaldehyde conversion at initial propionaldehyde concentration of 0.1 M in pure water and 80/20 GVL/H<sub>2</sub>O at 175°C using 50mg BEA, Y-SiO<sub>2</sub>/Al<sub>2</sub>O<sub>3</sub> ratio:15, Y-SiO<sub>2</sub>/Al<sub>2</sub>O<sub>3</sub> ratio:2.6, MFI, MOR, and FER as catalysts. Reactions were carried out in a batch reactor for 2 hours. Propionaldehyde conversion is shown in Figure 4.2-1 and selectivities to all reaction products are shown in Figure 4.2-3 for these reactions.

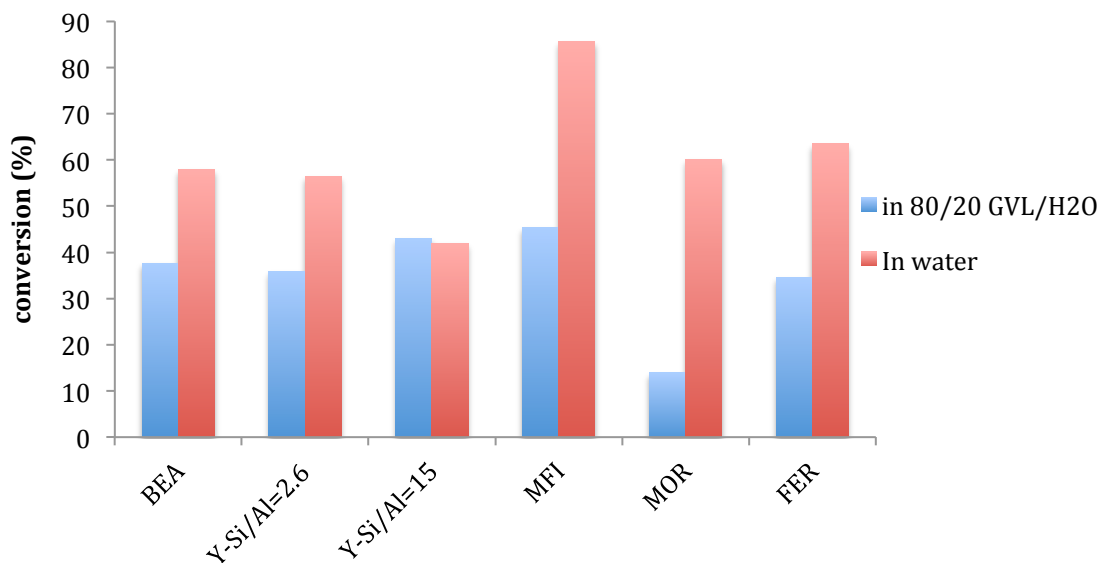


**Figure 4.2-1:** Conversions of propionaldehyde in the reaction of propionaldehyde with an initial concentration of 0.2 M, using BEA, Y-SiO<sub>2</sub>/Al<sub>2</sub>O<sub>3</sub> ratio:15, Y-SiO<sub>2</sub>/Al<sub>2</sub>O<sub>3</sub> ratio:2.6, MFI, MOR, and FER as catalyst in both solvents: GVL/H<sub>2</sub>O and pure water at 175°C for 2 hours.

GVL has a molecular structure shown in Figure 4.2-2. The molecular volume is 0.05631 m<sup>3</sup>/kmol<sup>[14]</sup>. The molecular size (diameter) is determined to be 5.63Å using the ball volume equation  $V = \frac{4}{3}\pi r^3$ . Channel sizes of the 5 types of zeolites are 6.31Å for FER, 6.36 Å for MFI, 6.68Å for BEA, 6.7 Å for MOR, and 11.24Å for Y<sup>[15]</sup>. All channel sizes of the 5 types of zeolites are larger than the GVL molecular size.

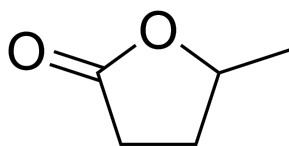


**Figure 4.2-2:** Molecular structure of  $\gamma$ -valerolactone (GVL)

The conversions of propionaldehyde were lower using GVL/H<sub>2</sub>O mixture as the solvent compared to pure water on all of the zeolites (except the higher Si/Al ratio Y zeolite). This apparent inhibition occurred to a lesser extent on the large pore zeolites (decreased from

57%-58% to 36%-37% on BEA and Y) than on the medium (decrease from 86% to 46% on MFI) and small pore (decrease from 60% to 14% on MOR and from 63% to 35% on FER). The more pronounced decrease in conversion of the smaller pore zeolites indicates that GVL molecules may be obstructing zeolite micropores and thus, preventing access of propionaldehyde molecules to acid sites.

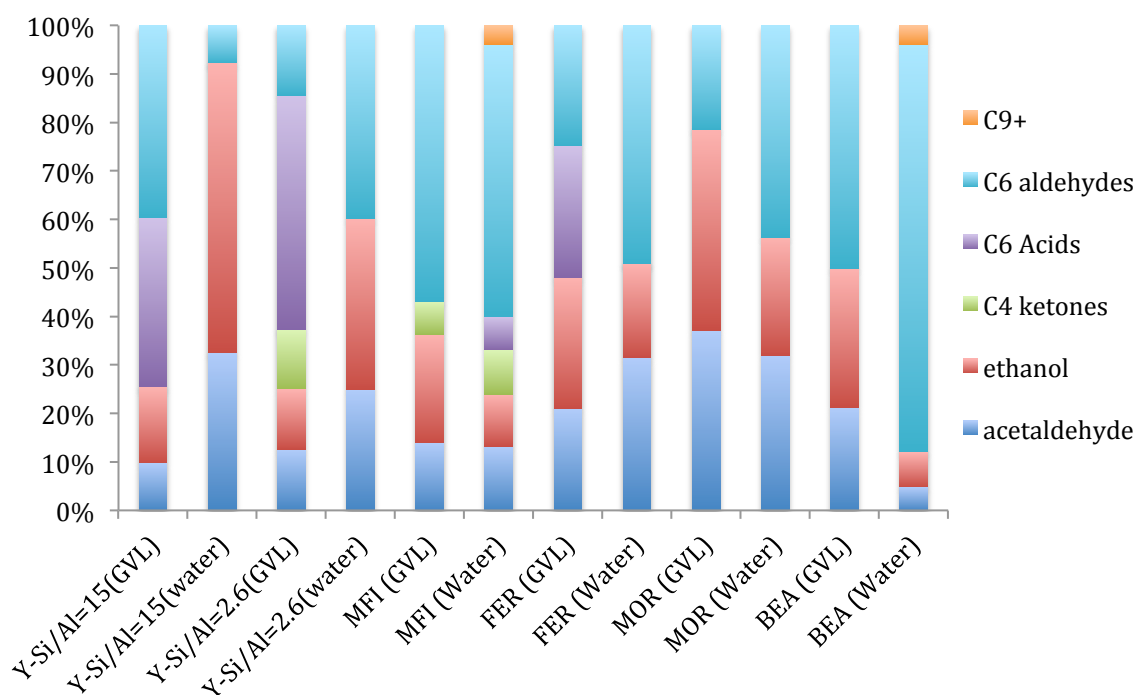


**Figure 4.2-3:** Selectivities to ethanol, acetaldehyde, C<sub>4</sub> ketones, C<sub>6</sub> acids, C<sub>6</sub> aldehydes, and C<sub>9</sub><sup>+</sup> in the reaction of propionaldehyde with an initial concentration of 0.2 M, using BEA, Y-SiO<sub>2</sub>/Al<sub>2</sub>O<sub>3</sub> ratio:15, Y-SiO<sub>2</sub>/Al<sub>2</sub>O<sub>3</sub> ratio:2.6, MFI, MOR, and FER as catalyst in both solvents: GVL/H<sub>2</sub>O and pure water at 175°C for 2 hours.

The selectivities shown in Figure 4.2-3 represent the predominant products formed during solid acid catalyzed propionaldehyde conversion (according to the reaction schematics shown in Figure 1-1). The aldol-condensation product (2-methyl-2-pentenal) forms with the highest selectivity on all but two of the catalysts tested and using both solvents (57% and 56% for MFI in GVL/H<sub>2</sub>O and in water respectively, 25% and 49% for FER in GVL/H<sub>2</sub>O and in

water respectively, 21% and 44% for MOR in GVL/H<sub>2</sub>O and in water respectively, 50% and 84% for BEA in GVL/H<sub>2</sub>O and in water respectively). All of the zeolites appear to facilitate cracking of C<sub>6</sub> aldehydes to form acetaldehyde and ethanol (to different extents) in both GVL/H<sub>2</sub>O and water solvents (25% and 93% for H-Y SiO<sub>2</sub>/Al<sub>2</sub>O<sub>3</sub> ratio:15 in GVL/H<sub>2</sub>O and water respectively, 25% and 60% for H-Y SiO<sub>2</sub>/Al<sub>2</sub>O<sub>3</sub> ratio:2.6 in GVL/H<sub>2</sub>O and water respectively, 36% and 24% for MFI in GVL/H<sub>2</sub>O and water respectively, 48% and 51% for FER in GVL/H<sub>2</sub>O and water respectively, 78% and 56% for MOR in GVL/H<sub>2</sub>O and water respectively, 50% and 12% for BEA in GVL/H<sub>2</sub>O and water respectively). The second product of cracking (C<sub>4</sub> hydrocarbons) is likely in the gas phase (which was not analyzed). The large/medium pore zeolites (BEA and MFI) exhibit the highest selectivity toward the condensation product (over cracking side reactions) possibly as a result from pore sizes that are too small to promote  $\beta$ -scission cracking (as found in Y) and too large to solvate protolytic cracking transition states (as found in MOR and FER). H-Y SiO<sub>2</sub>/Al<sub>2</sub>O<sub>3</sub> ratio:15 in water (8%) and H-Y SiO<sub>2</sub>/Al<sub>2</sub>O<sub>3</sub> ratio:2.6 in GVL/H<sub>2</sub>O (14%) exhibited low selectivities toward the condensation products in favor of oxidation and cracking reactions. C<sub>6</sub> acids such as 5-Hexenoic acid appear in H-Y SiO<sub>2</sub>/Al<sub>2</sub>O<sub>3</sub> ratio:15 (35% in GVL/H<sub>2</sub>O), H-Y SiO<sub>2</sub>/Al<sub>2</sub>O<sub>3</sub> ratio:2.6 (48% in GVL/H<sub>2</sub>O). The large cages of Y zeolites may facilitate these two reactions that require bi-molecular transition states. C<sub>9+</sub> molecules (primarily aromatics) form through the direct cyclization path from C<sub>9</sub> aldehydes that form from a second aldol-condensation reaction between 2-methyl-2-pentenal and propionaldehyde. Cyclization reactions occur on MFI (3.8% selectivity to aromatics) or BEA (3.9% selectivity to aromatics) as catalysts and

using water as solvent. Again, this selectivity to aromatics on medium-to-large pore zeolites is consistent with a stabilizing effect on monomolecular transition states involved in cyclization reactions.



## Chapter 5. Conclusion

In summary, acid catalyzed reaction of propionaldehyde were studied in the liquid phase using various catalysts. Under ambient conditions using a homogeneous HCl catalyst, GVL solvates aldol-condensation transition states leading to an increase in the reaction rate constant of ~40%. The reaction network appears to be strongly influenced by the micropore environment for heterogeneously catalyzed systems. Medium-to-large pore zeolites (BEA and MFI) favor aldol-condensation steps and exhibit the highest selectivity to 2-methyl-2-pentenal. Small pore (FER and MOR) and large pore (Y) zeolites favor reaction paths leading to ethanol and acetaldehyde. The formation of these C<sub>2</sub> species could be from cracking reactions that are promoted by large pores (for  $\beta$ -scission) and small pores (for protolytic cracking) within zeolites. The ultimate conclusion from this work is a basis for which future studies can be conducted. Bulk phase solvents appear to have less of an influence on reaction path for heterogeneously catalyzed systems (compared to homogeneous systems), and medium-to-large pore zeolites (such as BEA and MFI) appear to favor C-C bond formation paths that lead to the chain growth desired to upgrade short chain oxygenates to fuel range hydrocarbons.

## Reference

1. Bridgwater, A. V. (1999). Principles and practice of biomass fast pyrolysis processes for liquids. *Journal of Analytical and Applied Pyrolysis*, 51(1-2), pp. 3-22.
2. Putun, A. E., Ozcan, A., Gercel, H. F., Putun, E. (2001). Production of biocrudes from biomass in a fixed bed tubular reactor: product yields and compositions. *Fuel*, 80(10), pp. 1371-1378.
3. Saxena, R. C., Adhokari, D.K., Gotal, H.B. (2009). Biomass-based energy fuel through biochemical routes: A review. *Renewable and Sustainable Energy Reviews*, 13(1), pp. 167-178.
4. Alonso, D.M., Bond, J.Q., Dumesic, J.A. (2010). Catalytic conversion of biomass to biofuels. *Green Chemistry*, 12(9), pp. 1493-1513.
5. Luteracher, J.S., Rand, J.M., Alonso, D.M., Han, J., Youngquist, J. T., Maravelias, C.T., Pfleger, B. F., Dumesic, J.A. (2014). Nonenzymatic Sugar Production from Biomass Using Biomass-Derived  $\gamma$ -Valerolactone. *Science*, 343(6168), pp. 277-280.
6. Casale, M. T., Richman, A. R., Elrod, M. J., Garland, R. M., Beaver, M. R., Tolvert, M. A. (2007). Kinetics of acid-catalyzed aldol condensation reactions of aliphatic aldehydes. *Atmospheric Environment*, 41(29), pp. 6212-6224.
7. Alonso, D. M., Gallor, J. M. R., Mellmer, M. A., Wettstein, S. G., Dumesic, J. A. (2013). Direct conversion of cellulose to levulinic acid and gamma-valerolactone using solid acid catalysts. *Catalysis Science & Technology*, 3(4), pp. 927-931.
8. Zhang, L., Yu, H., Wang, P., Li, Y. (2014). Production of furfural from xylose, xylan and corncob in gamma-valerolactone using  $\text{FeCl}_3 \cdot 6\text{H}_2\text{O}$  as catalyst. *Bioresource Technology*, 151, pp. 355-360.
9. Qi, L., Mui, Y. F., Lo, S. W., Lui, M. Y., Akien, G. R., Horvath, I. T. (2014). Catalytic Conversion of Fructose, Glucose, and Sucrose to 5-(Hydroxymethyl)furfural and Levulinic and Formic Acids in  $\gamma$ -Valerolactone As a Green Solvent. *ACS Catalysis*, 4(5), pp. 1470-1477.
10. Mellmer, M.A., Alonso, D.M., Luterbacher, J. S., Gallo, J.M.R., Dumesic, J.A. (2014). Effects of  $\gamma$ -valerolactone in Hydrolysis of Lignocellulosic Biomass to Mono Saccharides. *Green Chemistry*, 16(11), pp. 4659-4662.

11. Mellmer, M.A., Sener, C., Gallo, J. M. R., Luterbacher, J. S., Alonso, D. M., Dumesic, J. A. (2014). Solvent Effects in Acid-Catalyzed Biomass Conversion Reactions. *Angewandte Chemie*, 53(44), pp. 11872-11875.
12. Lin F., Chin Y. (2016). Alkanal transfer hydrogenation catalyzed by solid Bronsted acid sites. *Journal of Catalysis*, 341, pp. 136-148.
13. McGrath, M. J., Kuo, W., Ngouana, B. F., Ghogomu, J. N., Mundy, C. J., Marenich, A. V., Cramer, C. J., Truhlar, D. G., Siepmann, J. I. (2013). Calculation of the Gibbs free energy of solvation and dissociation of HCl in water via Monte Carlo simulations and continuum solvation models. *Physical Chemistry Chemical Physics*, 15(32), pp. 13578-13585.
14. DIPPR Project 801 – Full Version. (2005, October 17). *Design Institute for Physical Property Research/AlChE*. Retrieved from [https://app.knovel.com/web/toc.v/cid:kpDIPPRPF7/viewerType:toc/root\\_slug:dippr-project-801-full/url\\_slug:front-matter?&issue\\_id=kpDIPPRPF7](https://app.knovel.com/web/toc.v/cid:kpDIPPRPF7/viewerType:toc/root_slug:dippr-project-801-full/url_slug:front-matter?&issue_id=kpDIPPRPF7)
15. Database of Zeolite Structures. (2017, March 17). Retrieved from <http://www.iza-structure.org/databases/>